Effects of crossed electric and magnetic fields on the electronic and excitonic states in bulk GaAs and GaAs/Ga$_{1-x}$Al$_x$As quantum wells

M. de Dios-Leyva,[1] C. A. Duque,[2] and L. E. Oliveira[3]

[1]*Department of Theoretical Physics, University of Havana, San Lázaro y L, Vedado 10400, Havana, Cuba*
[2]*Instituto de Física, Universidad de Antioquia, AA 1226, Medellín, Colombia*
[3]*Instituto de Física, Unicamp, CP 6165, Campinas-SP 13083-970, Brazil*

The variational procedure in the effective-mass and parabolic-band approximations is used in order to investigate the effects of crossed electric and in-plane magnetic fields on the electronic and exciton properties in semiconductor heterostructures. Calculations are performed for bulk GaAs and GaAs/Ga$_{1-x}$Al$_x$As quantum wells, for applied magnetic fields parallel to the layers and electric fields in the growth direction, and it is shown that the combined effects on the heterostructure properties of the applied crossed electric and magnetic fields and the direct coupling between the center-of-mass and internal exciton motions may be dealt with via a simple parameter representing the spatial distance between the centers of the electron and hole magnetic parabolas. Exciton properties are analyzed by using a simple hydrogenlike envelope excitonic wave function and present theoretical results are found in fair agreement with available experimental measurements on the diamagnetic shift of the photoluminescence peak position of GaAs/Ga$_{1-x}$Al$_x$As quantum wells under in-plane magnetic fields.

PACS number(s): 73.20.Mf, 71.55.Eq, 73.21.Fg

I. INTRODUCTION

In the last two decades or so, a considerable amount of both experimental and theoretical studies have been devoted to the understanding of a number of physical properties of semiconductor heterostructures and nanostructures. Such semiconductor systems are of significant importance for the development of electronic, optoelectronic, and spintronics devices. Of course, a detailed knowledge of the optical properties of semiconductor heterostructures may be of significance for device applications. In that respect, the study of exciton properties in those systems is of great importance, as such coupled electron-hole (*e-h*) excitations, which arise from the *e-h* Coulomb interaction, may considerably modify the interband optoelectronic properties of semiconductor heterostrutures. For a number of reasons, heterostructures such as GaAs/Ga$_{1-x}$Al$_x$As superlattices (SLs), quantum wells (QWs), quantum-well wires (QWWs), and quantum dots (QDs) constitute the semiconductor systems that have attracted the most attention in the literature. Here, we are most interested in the effect of excitonic excitations on the optoelectronic properties of GaAs/Ga$_{1-x}$Al$_x$As QWs. When the electron and hole carriers are confined in the same region of the direct space and in the same point of the inverse *k*-space, a large overlap of the single-particle wave functions occurs, and the excitation is called a direct exciton; alternatively, if the carriers are confined in different regions of the direct space and/or in different points of the inverse *k*-space, large changes in the physical properties may be observed due to the small electron-hole wave functions overlap, and the exciton is termed as an indirect exciton. Exciton effects on the optical spectrum of such systems usually consist of discrete states each having a dispersion that reflects the movement of the coupled *e-h* pair as a whole. As the photon momentum is quite small, $\lesssim 10^{-4}$ Å^{-1}, optical experimental studies usually would not give much information about the finite center-of-

mass (CM) momentum of exciton states. Studies in exciton dispersion and related properties have been recently performed both experimentally, through photoluminescence (PL) and magnetoabsorption experiments,[1–7] measurements of the Fano line shape for resonant states,[8] the exciton-mass dependence of the recombination time,[9] experimental data on polariton effects,[10,11] and recent PL measurements[12] of modulation-doped GaAs/AlGaAs QWs and heterojunctions, as well as theoretically.[13–24]

Evidences on the magnetic-field induced indirect fundamental band gap in modulation-doped In$_x$Ga$_{1-x}$As QWs (Ref. 1) and in-plane magnetic-field induced transitions in multiple GaAs/Ga$_{1-x}$Al$_x$As extremely-shallow QW heterostructures[2] have been experimentally reported. Whittaker *et al.*[1] have shown that the presence of the in-plane magnetic field may modify the nature of the subband structure due to the relationship between the in-plane momentum, perpendicular to the field, and the position of the orbit center on the growth axis, whereas Fritze *et al.*[2] suggested that extremely shallow QWs confine the exciton as a whole and observed a crossover from a three-dimensional to a two-dimensional-like exciton behavior associated with the dynamical coupling[13] of the CM and relative *e-h* motions, controlled by the in-plane magnetic field. Chang *et al.*[20] studied the quantum-confined magneto-Stark effect in a diluted-magnetic-semiconductor coupled-QW structure and reported a transition from the optical active exciton state to an indirect dark exciton state under increasing in-plane magnetic fields. Also, luminescence measurements of a GaAs/Ga$_{1-x}$Al$_x$As double QW under in-plane magnetic fields up to 22 T have been reported by Orlita *et al.*[5] They have studied the properties of spatially direct and indirect excitons and concluded that the dominating radiative recombination of localized indirect excitons does not allow one to observe the quenching of the spatially indirect exciton luminescence and the quadratic shift of their energy under in-plane magnetic fields,[4,6] with the conse-

quence that the possibility of an exciton dispersion engineering[3,4,19] would then be limited in these kinds of samples. By theoretically studying infinite-barrier GaAs QWs, under an externally applied electric field and a crossed strong in-plane magnetic field, Niculescu[23] found that the electric field breaks down the degeneracy of the states symmetrically positioned in *p*-space, and that, by controlling the values of the externally applied fields, one may enhance or reduce the energy and spatial separation of the electron and hole in the QW leading to a nonparabolic subband structure. It was then argued that this may be used to study single and multiple QW heterostructures without the need of the growth of many different samples. Moreover, combined theoretical and experimental studies from Ashkinadze *et al.*[12] for the effect of an in-plane magnetic field on the PL spectrum of modulation-doped heterostructures have suggested that there are remarkable spectral modifications of the PL spectra in both modulation-doped QWs and high-quality heterojunctions, due to $B_\parallel$-induced modifications in the direct optical transitions in QWs, and effects on the free holes in heterojunctions, respectively. Also, studies on the magnetic-field effects on indirect excitons[3,6,17,24] in coupled GaAs/(Ga,Al)As QWs reveal that the exciton effective mass is enhanced as the growth-direction magnetic field increases and, at high fields, it becomes larger than the sum of the *e* and *h* masses, suggesting that a magnetoexciton is an excitation with effective mass determined by the coupling[13] between the CM motion and internal structure rather than by the masses of its constituents. Recent theoretical calculations by Reyes *et al.*[24] suggest that the inclusion of both the effects of the finite-width barrier and well confining potentials as well as of the appropriate electronic band structure could be important for a realistic description of the experimental results.

The aim of the present work is to study the magneto-Stark effect for confined excitons in single GaAs/Ga1−xAlxAs QWs within a variational procedure in the effective-mass and parabolic band approximations. The magnetic field is considered perpendicular to the growth direction of the heterostructure, whereas the applied electric field is along the growth direction. It is demonstrated that the joint effects of the applied crossed electric and magnetic fields and the direct coupling between the center-of-mass and internal exciton motions may be dealt with via a simple parameter representing the spatial distance between the centers of the electron and hole magnetic parabolas. We note that the present study, although very much related to the previous theoretical work by Reyes *et al.*,[24] in fact describes a substantially different physical situation: previously we dealt with coupled GaAs/Ga1−xAlxAs QWs under magnetic fields applied perpendicular to the layers, with the additional assumption that the electron and hole forming the exciton were considered confined either in the same plane or in different planes, whereas in the present work we are concerned with a semiconductor heterostructure under crossed electric and magnetic applied fields, and proper consideration is taken of the finite well widths and confinement along the *z*-growth direction. Moreover, the exciton variational wave function, in the effective-mass approximation, is considered in some detail, with some results presented within a hydrogeniclike variational wave function depending on one, two, or three variational parameters. Here we emphasize that, although the present calculations are performed for GaAs/Ga1−xAlxAs QWs, the present theoretical framework may be straightforwardly generalized to apply for a general semiconductor heterostructure, and, in that respect, it constitutes a major advance with respect to our previous study.[24] Also, we note that Coli and Bajaj[25] used a many-body approach in order to calculate the exciton binding energies in semiconductor QWs over a large range of QW widths, and their results were found in very good agreement with those obtained by Antonelli *et al.*[26] who used a variational approach. Moreover, the effective-mass and parabolic approximations have been used quite successful in the understanding of experimental measurements related to shallow Coulomb-bound states[27–29] (shallow donors, acceptors, and excitons) in GaAs/Ga1−xAlxAs QWs and QWWs. The paper is organized as follows. In Sec. II we detail the present theoretical approach. Section III is concerned with the results and discussion, and finally, our conclusions are given in Sec. IV.

II. THEORETICAL FRAMEWORK

In the present study, we are concerned with the properties of heavy-hole exciton states in a semiconductor GaAs/Ga1−xAlxAs heterostructure, grown along the *z* axis, under applied magnetic ($\vec{B}$) and electric ($\vec{E}$) fields. Here, for simplicity, we will work within the effective-mass and nondegenerate-parabolic band approximations. Therefore the Hamiltonian for the exciton may be given by

$$\hat{H} = \frac{1}{2m_e^*}\left(\hat{\vec{p}}_e + \frac{e}{c}\vec{A}_e\right)^2 + \frac{1}{2m_h^*}\left(\hat{\vec{p}}_h - \frac{e}{c}\vec{A}_h\right)^2 + V_e(z_e) + V_h(z_h)$$

$$- \frac{e^2}{\epsilon|\vec{r}_e - \vec{r}_h|} + e\vec{E}\cdot(\vec{r}_e - \vec{r}_h), \qquad (1)$$

where $\vec{A}_e = \vec{A}(\vec{r}_e)$ and $\vec{A}_h = \vec{A}(\vec{r}_h)$ are the vector potentials associated to the magnetic field, $\hat{\vec{p}}_e$, $\hat{\vec{p}}_h$ and m_e^*, m_h^* are the momentum operators and the effective masses of the electron and heavy hole, respectively, V_e and V_h are the electron and hole confining potentials, respectively, *e* is the absolute value of the electron charge, and ϵ is the dielectric constant. The above-mentioned parameters for bulk GaAs and Ga1−xAlxAs barrier were taken at low temperatures from the data collected by Li.[30] For the dielectric constants and electron and heavy-hole effective masses, we have considered the same values as in GaAs throughout the heterostructure.[31]

As the heterostructure is grown along the *z* direction, the Schrödinger equation with the above Hamiltonian is invariant under simultaneous translation of both the *e* and *h* coordinates parallel to the (x, y) plane and the corresponding gauge transformation, which leads to the conservation of the $\hat{\vec{P}} = (\hat{P}_x, \hat{P}_y)$ transverse components of the exciton CM magnetic momentum.[13,24] By choosing the in-plane applied magnetic field along the *x* direction, $\vec{B} = B\hat{x}$, using the Landau gauge $\vec{A}(\vec{r}) = -zB\hat{y}$, and a crossed electric field in the growth direction, $\vec{E} = -E\hat{z}$, one may write the common eigenfunctions of both $\hat{H}$ and $\hat{\vec{P}}$ as

$$\Psi_{exc}(\vec{r}_e, \vec{r}_h) = \frac{\exp\left(\frac{i}{\hbar}\vec{P}\cdot\vec{R}\right)}{\sqrt{S}}\Phi(\vec{\rho}, z_e, z_h), \qquad (2)$$

where $\vec{P} = \hbar\vec{K}$ is the two-component eigenvalue of the exciton transverse CM $\hat{\vec{P}}$ magnetic momentum, $\vec{R} = \frac{1}{M}(m_e^*\vec{\rho}_e + m_h^*\vec{\rho}_h)$ is the in-plane exciton CM coordinate, $M = m_e^* + m_h^*$ is the total exciton mass, S is the $x-y$ transverse area of the heterostructure, $\vec{\rho} = \vec{\rho}_e - \vec{\rho}_h$ is the in-plane internal exciton coordinate, and $\Phi(\vec{\rho}, z_e, z_h)$ (with corresponding exciton energy E_X) is the eigenfunction of

$$\hat{H} = \hat{H}_0 - \frac{e^2}{\epsilon|\vec{r}_e - \vec{r}_h|}, \qquad (3)$$

where

$$\hat{H}_0 = \frac{\hat{p}_{ez}^2}{2m_e^*} + V_e(z_e) + \frac{\hat{p}_{hz}^2}{2m_h^*} + V_h(z_h) + \hat{h}, \qquad (4)$$

with

$$\hat{h} = \frac{1}{2m_e^*}\left[\frac{m_e^*}{M}\vec{P} + \hat{\vec{p}}_\rho + z_e\vec{\mu}\right]^2 + \frac{1}{2m_h^*}\left[\frac{m_h^*}{M}\vec{P} - \hat{\vec{p}}_\rho - z_h\vec{\mu}\right]^2 - eE(z_e - z_h), \qquad (5)$$

$\hat{\vec{p}}_\rho = -i\hbar\nabla_\rho$, and $\vec{\mu} = -\frac{eB}{c}\hat{y}$. In order to find the exciton eigenfunctions, we first obtain the eigenfunctions of $\hat{H}_0$, by ignoring the e-h Coulomb interaction in Eq. (3), and write

$$\hat{H}_0\Phi_0 = E_0\Phi_0. \qquad (6)$$

As before, due to the translational invariance of $\hat{H}_0$ in the (x,y) plane, the $\hat{\vec{p}}_\rho$ noncorrelated e-h pair transverse momentum is conserved, and one may write the eigenfunction of Eq. (6) as

$$\Phi_0 = \frac{\exp(i\vec{k}\cdot\vec{\rho})}{\sqrt{S}}F(z_e, z_h), \qquad (7)$$

where $\vec{p} = \hbar\vec{k}$ is a two-component eigenvalue of $\hat{\vec{p}}_\rho$ and $F(z_e, z_h)$ is the eigenfunction of the Hamiltonian

$$\hat{H}_0 = \frac{P_x^2}{2M} + \frac{p_x^2}{2\mu} - K_y l_B(eEl_B) - \frac{(eEl_B)^2}{2\beta_0} + \frac{\hat{p}_{ez}^2}{2m_e^*} + V_e(z_e)$$
$$+ \frac{1}{2}m_e^*\omega_e^2(z_e - z_e^0)^2 + \frac{\hat{p}_{hz}^2}{2m_h^*} + V_h(z_h) + \frac{1}{2}m_h^*\omega_h^2(z_h - z_h^0)^2, \qquad (8)$$

corresponding to the eigenvalue

$$E_0 = \frac{P_x^2}{2M} + \frac{p_x^2}{2\mu} - K_y l_B(eEl_B) - \frac{(eEl_B)^2}{2\beta_0} + E_\eta^e(z_e^0) + E_\alpha^h(z_h^0), \qquad (9)$$

where η, $\alpha = 0,1,2,3\ldots$ are the Landau magnetic subband indices, $\beta_0 = \frac{\hbar^2}{Ml_B^2}$, $l_B = \sqrt{\frac{\hbar c}{eB}}$ is the Landau magnetic length (or cyclotron radius), μ is the e-h reduced mass,

$$z_{e,h}^0 = \frac{c}{eB}\left(p_y \pm \frac{m_{e,h}^*}{M}P_y\right) \pm \frac{eE}{m_{e,h}^*\omega_{e,h}^2} \qquad (10)$$

are the noncorrelated e and h orbit-center positions along the growth direction, and $\omega_{e,h} = \frac{eB}{m_{e,h}^*c}$ are the corresponding cyclotron frequencies. Note that

$$\Delta = z_e^0 - z_h^0 = l_B\left(K_y l_B + \frac{eEl_B}{\beta_0}\right) \qquad (11)$$

represents the spatial distance between the centers of the noncorrelated electron and hole magnetic parabolas,[13] and is given by the magnitude of the vector $\vec{\rho}_0 = \frac{c}{eB^2}\vec{B}\times\left(\vec{P} + \frac{Mc}{B^2}\vec{B}\times\vec{E}\right)$, which connects the two local minima associated with the e-h Coulomb interaction and the effective magnetic parabolic potential.

The above result for the noncorrelated e-h pair allows one to variationally obtain the ground-state exciton energy and corresponding eigenfunction. The trial envelope variational wave function is chosen as

$$\Phi = \Phi_0(\vec{\rho}, z_e, z_h)f(\vec{r}), \qquad (12)$$

with $\vec{r} = \vec{r}_e - \vec{r}_h$,

$$f(\vec{r}) \propto e^{-\lambda r} \qquad (13)$$

is a hydrogenic $1s$-like wave function and λ is a variational parameter.[33] The exciton binding energy is given as $E_b = E_0^{gs} - E_X$, where E_0^{gs} is the ground-state energy associated to the noncorrelated e-h pair [cf. Eqs. (6) and (9)], which depends on the confining heterostructure potentials, applied electric and magnetic fields, and $K_y = P_y/\hbar$. The E_0^{gs} ground-state energy is obtained from Eq. (9), with η, $\alpha = 0$, through a minimization procedure with respect to z_e^0 or z_h^0, for a given value of $\Delta = z_e^0 - z_h^0$ [cf. Eq. (11)]. By using the corresponding $F_{gs}(z_e, z_h)$ ground-state eigenfunction of $\hat{H}_0$ [see Eq. (8)], we now define

$$h(z_e, z_h) = F_{gs}^2(z_e, z_h), \qquad (14)$$

$$g(z) = \int_{-\infty}^{+\infty} h(z_e, z_h)dZ, \qquad (15)$$

where $Z = \frac{m_e z_e + m_h z_h}{M}$ is the z-direction CM coordinate, and $z = z_e - z_h$ is the corresponding e-h distance in the growth direction, and straightforwardly obtain the binding energy through a maximization (variational) procedure of

$$E_b(\lambda) = -\frac{\hbar^2\lambda^2}{2\mu} + \frac{\frac{e^2}{\varepsilon}\int\frac{gf^2}{r}d^3\vec{r}}{\int gf^2 d^3\vec{r}}. \qquad (16)$$

Here we note that, for bulk GaAs, there are no confining potentials, one obtains

$$E_0^{gs} = \frac{P_x^2}{2M} + \frac{p_x^2}{2\mu} - K_y l_B(eEl_B) - \frac{(eEl_B)^2}{2\varepsilon_0} + \frac{\hbar\omega_{exc}}{2}, \qquad (17)$$

with $\omega_{exc} = \frac{eB}{\mu c}$,

$$F_{gs}(z_e,z_h) = \frac{1}{\sqrt{\sqrt{\pi}l_B}} \exp\left[-\frac{(z_e-z_e^0)^2}{2l_B^2}\right]$$
$$\times \frac{1}{\sqrt{\sqrt{\pi}l_B}} \exp\left[-\frac{(z_h-z_h^0)^2}{2l_B^2}\right], \qquad (18)$$

and therefore Eq. (15) reduces to

$$g(z) = \frac{1}{\sqrt{2\pi}l_B} \exp\left[-\frac{(z-\Delta)^2}{2l_B^2}\right], \qquad (19)$$

which may be used in Eq. (16) in order to obtain the E_b exciton binding energy in bulk GaAs.

In the case of a semiconductor GaAs/Ga$_{1-x}$Al$_x$As heterostructure grown along the z axis, the determination of the eigenfunctions and eigenvalues of Eq. (8) involves a simple characteristic problem for the electron (or hole), associated with the Hamiltonian

$$\hat{H}_{e,h} = -\frac{\hbar^2}{2m_{e,h}^*}\frac{d^2}{dz^2} + \frac{1}{2}m_{e,h}^*\omega_{e,h}^2(z-z_{e,h}^0)^2 + V_{e,h}(z), \quad (20)$$

which may be readily solved via an expansion in terms of sine[34] or harmonic-oscillator[35] functions.

Finally, in the quantitative study of the optical properties of excitons in semiconductor heterostructures, it is necessary to evaluate the matrix elements for the interband optical transitions, which (by neglecting the photon wave vector) are proportional to[15]

$$\int \Psi_{exc}(\vec{r}_e = \vec{r}, \vec{r}_h = \vec{r})d^3\vec{r} = \delta_{\vec{K},0}I_{overlap}, \qquad (21)$$

where $\vec{K}$ is the exciton wave vector [cf. Eqs. (2), (7), and (12)], and

$$I_{overlap} = \sqrt{S}\int_{-\infty}^{+\infty}\Phi(\vec{\rho}=0,z_e=z_h=z)dz \qquad (22)$$

defines the e-h overlap integral. Later on, we will devote special attention to the quantitative study of this magnitude.

III. RESULTS AND DISCUSSION

Due to the importance of the Δ parameter in the study of the exciton states in GaAs/Ga$_{1-x}$Al$_x$As semiconductor heterostructures under growth-direction applied electric (E) and in-plane magnetic (B) fields, we show in Fig. 1 the relation between Δ, E, and B, contained in Eq. (11), for $K_y=0$. It follows that Δ, the spatial distance between the centers of the electron and hole magnetic parabolas, for a fixed value of the in-plane magnetic field [see Fig. 1(a)], is an increasing (linear, as $\Delta \sim E$) function of the growth-direction applied electric field. This is the expected result as the applied electric field tends to spatially separate or polarize the e-h pair. Notice, however, that as $\Delta = eEl_B^2/\beta_0 \sim E/B^2$, for a fixed value of E [cf. Fig. 1(b)], is a decreasing function of the magnetic field, the effect of increasing B is to reduce the separation or the polarization of the e-h pair, as the cyclotron radius is reduced. We believe this last result may be used to under-
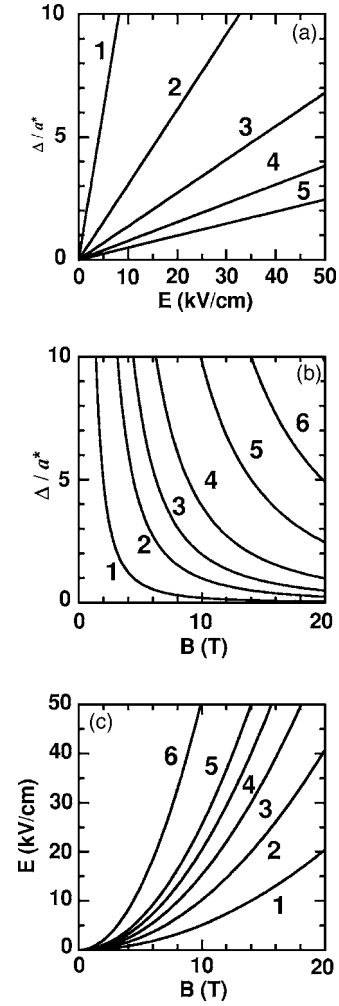

FIG. 1. Results obtained from Eq. (11) for $K_y=0$, by using the bulk GaAs parameters (see text): (a) Δ/a^* as a function of the growth-direction applied electric field, for various crossed-direction in-plane applied magnetic fields (1: $B=4$ T; 2: $B=8$ T; 3: $B=12$ T; 4: $B=16$ T; 5: $B=20$ T); (b) magnetic-field dependence of the spatial distance Δ between the centers of the electron and heavy-hole magnetic parabolas, for various values of the crossed-direction (growth-direction) applied electric field. The Δ distance is given in units of the $a^*=118$ Å heavy-hole exciton Bohr radius (1: $E=1$ kV/cm; 2: $E=5$ kV/cm; 3: $E=10$ kV/cm; 4: $E=20$ kV/cm; 5: $E=50$ kV/cm; 6: $E=100$ kV/cm); (c) magnetic-field dependence of the crossed-direction (growth-direction) applied electric field for fixed values of the Δ parameter (1: $\Delta/a^*=1$; 2: $\Delta/a^*=2$; 3: $\Delta/a^*=3$; 4: $\Delta/a^*=4$; 5: $\Delta/a^*=5$; 6: $\Delta/a^*=10$).

stand the physical mechanism responsible for the increase in the e-h wave-function overlap with increasing magnetic field, as suggested recently to explain the modification of the PL spectrum of high-quality heterojunctions[12] for filling factors $\nu < 2$. Moreover, note that $\Delta \to \infty$ when $B \to 0$ for each value of $E \neq 0$, which is due to the fact that the electric field tends to ionize the e-h pair in the limit of vanishing magnetic field. Figure 1(c) shows that the electric field is a parabolic function of the magnetic field for given value of the spatial separation between the electron and hole magnetic parabolas. Of course, a similar analysis and discussion may be carried out for $K_y \neq 0$. Note that, as we have considered $E \geq 0$ in Fig.
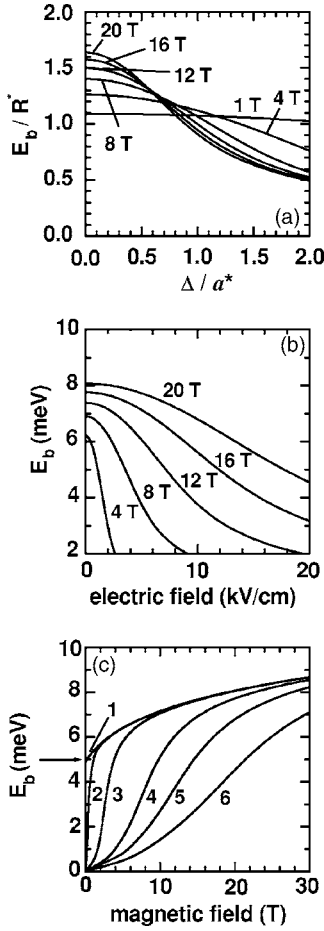
FIG. 2. Heavy-hole E_b exciton binding energies, for bulk GaAs, under crossed electric and magnetic fields, as functions of (a) the spatial distance Δ/a^* between the centers of the electron- and heavy-hole magnetic parabolas, (b) applied electric field, and (c) applied magnetic field. In (a), Δ is given in units of the exciton effective Bohr radius ($a^*=118$ Å) and the binding energy is in units of the heavy-hole exciton Rydberg ($R^*=4.9$ meV). In (c) curves 1–6 correspond to $E=0$, $E=0.1$ kV/cm, $E=1$ kV/cm, $E=5$ kV/cm, $E=10$ kV/cm, and $E=20$ kV/cm, respectively. The arrow at $E=B=0$ in (c) indicates the bulk GaAs value of the exciton binding energy. Results in (b) and (c) correspond to $K_y=0$ (see text).

1, then $\Delta \geqslant 0$. In the following, for simplicity, we will only consider this range of values of E and Δ even when $K_y \neq 0$.

A. Electronic and exciton states in bulk GaAs

We first present the calculated results for bulk GaAs under a $(-z)$-direction applied electric field and x-direction magnetic field, i.e., under crossed electric and magnetic fields. We then display in Figs. 2–4, for bulk GaAs, the heavy-hole exciton binding energy E_b, the average e-h distance $\langle z_e - z_h \rangle$ along the z direction, and the e-h overlap integral I_{overlap}, as functions of the spatial distance Δ between the centers of the electron and heavy-hole magnetic parabolas, and applied electric and magnetic fields. As one can see from Figs. 2(a) and 2(b), for a fixed value of the magnetic field, the exciton
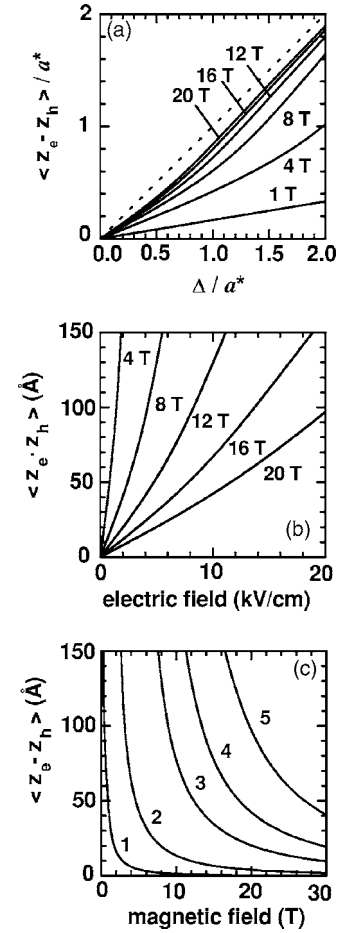
FIG. 3. Average e-h distance $\langle z_e - z_h \rangle$ along the z direction, for an exciton in bulk GaAs, under crossed electric and magnetic fields, as functions of (a) the spatial distance Δ/a^* between the centers of the electron- and heavy-hole magnetic parabolas, (b) applied electric field, and (c) applied magnetic field. In (c) curves 1–5 correspond to $E=0.1$ kV/cm, $E=1$ kV/cm, $E=5$ kV/cm, $E=10$ kV/cm, and $E=20$ kV/cm, respectively. The dashed line in (a) corresponds to the representation of $\langle z_e - z_h \rangle = \Delta$, and results in (b) and (c) are for $K_y=0$ (see text).

binding energy is a decreasing function of the Δ parameter and applied electric field, respectively [notice that Δ, E, and B are related via Eq. (11)]. This result may be understood as follows. As in the bulk the noncorrelated electron and hole oscillate around the z_e^0 and z_h^0, respectively, and the binding energy is determined by the e-h attractive Coulomb interaction, which tends to zero with the e-h distance, it is obvious that E_b, for a fixed value of B, must diminish with both the $\Delta = z_e^0 - z_h^0$ parameter or with the applied electric field $E \sim B^2 \Delta$ [see Eq. (11) with $K_y=0$]. As expected,[36] the present calculations for $\Delta=0$ and $E=0$ show an increase in the exciton binding energy as one increases the strength of the applied magnetic field, i.e., as the confinement effects due to the magnetic field increases. On the other hand, note in Fig. 2(a) that E_b decreases with increasing values of the applied magnetic field for relatively high (fixed) values of Δ. This behavior is due to the increasing confinement, for a fixed value of Δ, of the electron and hole around their corresponding equilibrium positions (near z_e^0 and z_h^0, respectively) as the
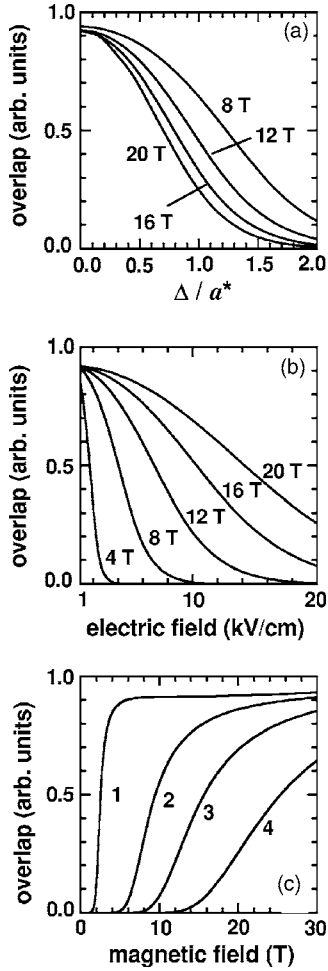
FIG. 4. *e-h* overlap integral $I_{overlap}$, for bulk GaAs, under crossed electric and magnetic fields, as functions of (a) the spatial distance Δ/a^* between the centers of the electron- and heavy-hole magnetic parabolas, (b) applied electric field, and (c) applied magnetic field. In (c) curves 1–4 correspond to $E=1$ kV/cm, $E=5$ kV/cm, $E=10$ kV/cm, and $E=20$ kV/cm, respectively. Results in (b) and (c) correspond to $K_y=0$ (see text).

magnetic field increases. With respect to the theoretical results presented in Fig. 2(a), it is interesting to notice the following: as the exciton binding energy is given as a function of the parameter $\Delta=(el_B^2/\beta_0)\widetilde{E}$, with $\widetilde{E}=E+\beta_0K_y/e$, these results describe the exciton K_y dispersion for a fixed applied electric field, and E_b as function of the parameter $\Delta=eEl_B^2/\beta_0$, or applied electric field, for $K_y=0$. Note that $\widetilde{E}$ is the effective electric field acting on the *e-h* pair, which is the sum of the externally applied field E, and electric field β_0K_y/e, which is felt in the CM frame of the *e-h* pair moving in the externally applied magnetic field.[13,17] Moreover, as for $K_y=0$ the applied electric field is related to the spatial separation Δ between the electron and hole magnetic parabolas by the relation $E=\beta_0\Delta/(el_B^2)\sim B^2\Delta$, it is obvious that Δ decreases with increasing B for a given value of E and therefore the binding energy must increase as B increases, for a fixed applied electric field, as shown in Fig. 2(b). The magnetic-field dependence of the exciton binding energy, shown in Fig. 2(c), clearly indicates that, in the absence of

applied electric or magnetic fields, the exciton binding energy goes to the bulk GaAs value [note the arrow at $E=B=0$ in Fig. 2(c)], and increases with the applied magnetic field as confining effects due to the field increases [see curve 1 in Fig. 2(c)]. Also note that, for $E\neq0$, the E_b exciton binding energy tend to zero as $B\rightarrow0$ $(\Delta\rightarrow\infty)$: As the *e-h* pair, in bulk GaAs, is in the presence of an applied electric field, both the electron and the hole are free to move in the system, and the exciton is unbound. The decrease of E_b with increasing E, for a fixed value of B, is of course due to the increase of $\Delta\sim E/B^2$ with the strength of the electric field.

In Fig. 3, we display the results of the present theoretical calculations for the average *e-h* distance in the *z* direction, for an exciton in bulk GaAs, as functions of Δ and applied electric and magnetic fields. Calculations were carried out by substituting the bulk function $g(z)$ [see Eq. (19)] into

$$\langle z_e - z_h \rangle = \int (z_e - z_h)|\Psi_{exc}(\vec{r}_e,\vec{r}_h)|^2 d^3\vec{r}_e d^3\vec{r}_h$$

$$= \frac{\int zg(z)\exp^{-2\lambda r}d^3\vec{r}}{\int g(z)\exp^{-2\lambda r}d^3\vec{r}}, \tag{23}$$

where $\Psi_{exc}(\vec{r}_e,\vec{r}_h)$ is the ground-state exciton wave function. Of course, $\langle z_e-z_h\rangle$ may also be straightforwardly evaluated for GaAs/Ga$_{1-x}$Al$_x$As semiconductor heterostructures by using the corresponding $g(z)$ function [see Eq. (15)]. As shown in Figs. 3(a) and 3(b), $\langle z_e-z_h\rangle=0$ for $\Delta=0$ and $E\sim B^2\Delta=0$ for a finite value of the magnetic field, as one would expect. This also follows from Eq. (23), for $B\neq0$, if one notes that the bulk $g(z)$ function [Eq. (19)] is an even function of *z* for $\Delta=0$ and $E=0$. Moreover, the other properties of the average *e-h* distance displayed in Fig. 3(a) may be understood as follows: (i) as z_e^0 and z_h^0 are, respectively, the oscillation centers of the noncorrelated electron and hole in the bulk, it is obvious that $\langle z_e-z_h\rangle=z_e^0-z_h^0=\Delta$ for the noncorrelated *e-h* pair, and $\langle z_e-z_h\rangle<\Delta$ [see full curves in Fig. 3(a)] for the correlated *e-h* pair, as the corresponding Coulomb interaction is attractive; (ii) as the *e-h* Coulomb interaction tends to zero as $\Delta\rightarrow\infty$, it is evident that $\langle z_e-z_h\rangle\rightarrow\Delta$ in the limit of high Δ [see each full curve in Fig. 3(a)]; (iii) as $(z-\Delta)^2/2l_B^2$ in the exponent of the bulk $g(z)$ function is proportional to $B(z-\Delta)^2$, the main contribution to the two integrals in Eq. (23), for high magnetic fields, comes from a small region around $z=\Delta$, and therefore $\langle z_e-z_h\rangle\rightarrow\Delta$ and the full curves in Fig. 3(a) tend to the dashed line as B increases. As shown in Fig. 3(b), the average *e-h* distance $\langle z_e-z_h\rangle$ increases with $E\sim B^2\Delta$, for a fixed value of B, as the Δ spatial separation between the magnetic parabolas increases with the applied electric field. As also shown in Figs. 3(b) and 3(c), $\langle z_e-z_h\rangle$ decreases with increasing values of the applied magnetic field, for fixed E, as $\Delta\sim E/B^2$ decreases with increasing strengths of the magnetic field.

The *e-h* overlap integral, for an exciton in bulk GaAs, as a function of Δ and crossed electric and magnetic fields, is depicted in Fig. 4. The rapid decrease of $I_{overlap}$ with Δ and E

observed in each curve of Figs. 4(a) and 4(b), respectively, is due to the fact that the *e-h* distance in the *z* direction increases with Δ, for a fixed applied magnetic field. This conclusion is, of course, in agreement with the analytical expression for the *e-h* overlap integral, which may be obtained from Eq. (22) and the corresponding ground-state solution $\Phi(\vec{\rho}, z_e, z_h)$ derived above for the bulk GaAs [see Eqs. (7), (12), (13), and (18)], i.e.,

$$I_{\text{overlap}} \propto e^{-\Delta^2/4l_B^2}. \tag{24}$$

Notice that the *e-h* overlap integral decreases with increasing strengths of the applied magnetic field for a fixed value of Δ [see Fig. 4(a)], whereas it increases with *B* for a given value of the applied electric field [see Figs. 4(b) and 4(c)]. This may be understood if one notes that Δ^2/l_B^2 in Eq. (24) must be taken as proportional to $B\Delta^2$ or E^2/B^3 in the analysis of the results presented in Fig. 4(a) and Figs. 4(b) and 4(c), respectively. Also, by taking into account, for $K_y = 0$, the relation $\Delta \sim E/B^2$ between the Δ spatial separation between the magnetic parabolas and the externally applied electric and magnetic fields, one obtains that, for a fixed value of the applied electric field, Δ decreases as the value of *B* increases. Therefore the attractive Coulomb interaction becomes stronger, and as a consequence both the exciton binding energy and *e-h* overlap integral should increase [see Figs. 2(c) and 4(c)]. Again, for $E \neq 0$, I_{overlap} tend to zero as $B \rightarrow 0$ ($\Delta \rightarrow \infty$), as the *e-h* pair is in the presence of an applied electric field, and the exciton is unbound. Also, it is interesting to note that the magnetic-field dependence of the *e-h* overlap integral, established above, for $K_y = 0$ and a fixed value of *E*, is essentially the same physical effect associated to the modification of the PL spectrum of high-quality heterojunctions[12] for filling factors $\nu < 2$, as mentioned before.

B. Electronic and exciton states in GaAs/Ga$_{1-x}$Al$_x$As QWs

We now turn to the study of the effects of crossed growth-direction electric *E* and in-plane magnetic *B* fields on the exciton states in GaAs/Ga$_{1-x}$Al$_x$As QWs. Figure 5 displays the ground-state magnetic subbands $E_e = E_0^e(z_e^0)$ and $E_h = E_0^h(z_e^0 - \Delta)$ [see Eq. (9)] associated with the noncorrelated electron and heavy hole, respectively, as functions of the z_e^0 center of the electron parabola, for an $L = 100$-Å GaAs/Ga$_{0.7}$Al$_{0.3}$As QW in the presence of a $B = 10$-T in-plane applied magnetic field, and for various values of the parameter $\Delta = z_e^0 - z_h^0$. Also depicted in Fig. 5 is the sum [cf. Eq. (9)] of the electron- E_e and heavy-hole E_h energies (dashed curves in Fig. 5). The arrow in each figure indicates the position of Δ in the z_e^0 axis. Moreover, Eq. (11) determines, for *B* and Δ given, the corresponding relation between the growth-direction electric field *E* and exciton K_y CM momentum. Note that in each one of these figures, where Δ is given, the value $z_{e,m}^0$ of z_e^0 corresponding to the minimum of $E_e + E_h$ determines the exact spatial position of the centers of the electron and heavy-hole ($z_{h,m}^0 = z_{e,m}^0 - \Delta$) magnetic parabolas. This allows us to obtain the noncorrelated *e-h* eigenfunction $F_{gs}(z_e, z_h)$ of the Hamiltonian (8) associated to the corresponding noncorrelated *e-h* ground-state
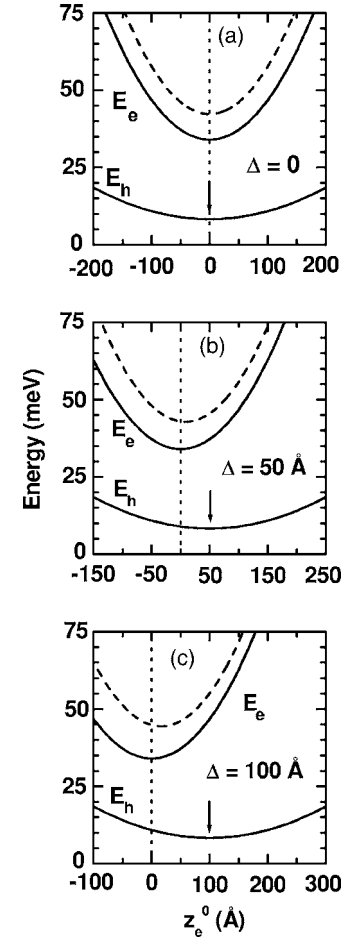

FIG. 5. z_e^0 dependence of the ground-state magnetic subbands $E_e = E_0^e(z_e^0)$ and $E_h = E_0^h(z_e^0 - \Delta)$ [see Eq. (9)] associated with the non-correlated electron and heavy hole, respectively, for an $L = 100$-Å GaAs/Ga$_{0.7}$Al$_{0.3}$As QW in the presence of a $B = 10$ T in-plane applied magnetic field, and for various values of the Δ parameter. The dashed curve represents the sum of the E_e electron- and E_h heavy-hole energies. The values of the corresponding growth-direction applied electric field and exciton K_y CM momentum are related to Δ via Eq. (11), for $B = 10$ T.

energy E_0^{gs}. With this observation, we stress the fundamental role played by Δ and $z_{e,m}^0$ in the determination of the exciton states in GaAs/Ga$_{0.7}$Al$_{0.3}$As semiconductor heterostructures. Also, it is important to note the following: as $z_{e,m}^0$ is the solution of the equation

$$\frac{dE_0^e(z_e^0)}{dz_e^0} + \frac{dE_0^h(z_e^0 - \Delta)}{dz_e^0} = 0 \tag{25}$$

and the first term in this expression reaches finite values greater that the absolute value of the second one for all z_e^0, $\Delta > 0$, it is obvious that when Δ increases from zero, $z_{e,m}^0$ also increases from zero, reaches its maximum value, and then starts decreasing to zero due to the fact that the second term in the above expression tends to zero as $\Delta \rightarrow \infty$ (not shown in Fig. 5). This means that when $\Delta > 0$ is increased, the center of the electron magnetic parabola remains enclosed, and the center $z_{h,m}^0 = z_{e,m}^0 - \Delta$ of the hole magnetic pa-
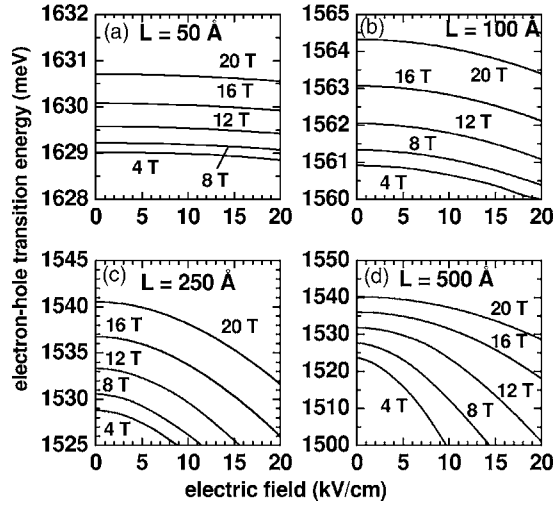
FIG. 6. Noncorrelated *e-h* energy transitions (for $K_y=0$) as functions of the growth-direction applied electric field, for GaAs/Ga$_{0.7}$Al$_{0.3}$As QWs of different L well widths and various values of the in-plane applied magnetic field.

FIG. 7. Heavy-hole exciton binding energy, in units of the heavy-hole exciton Rydberg $R^*=4.9$ meV, as a function of the spatial distance Δ/a^* ($a^*=118$ Å is the heavy-hole exciton effective Bohr radius) between the centers of the electron- and heavy-hole magnetic parabolas, for GaAs/Ga$_{0.7}$Al$_{0.3}$As QWs of different L well widths, and for various values of the in-plane magnetic field. The values of the corresponding growth-direction applied electric field and exciton K_y CM momentum are related to Δ and B via Eq. (11).

rabola shifts to $-\infty$. Taking into account the preceding observations and Eq. (9), for $P_x=p_x=\hbar K_y=0$, we have calculated (see Fig. 6) the E_0^{gs} noncorrelated *e-h* transition energies as functions of the growth-direction applied electric field, for GaAs/Ga$_{0.7}$Al$_{0.3}$As QWs of different L well widths and various values of the B in-plane applied magnetic field. The present calculation shows an increase in the noncorrelated transition energy as the electron and hole confinement increases, i.e., with the decreasing width of the QW or, alternatively, with the increasing strength of the applied in-plane magnetic field. The evolution of the applied electric-field dependence of the noncorrelated E_0^{gs} transition energy when the well width goes from $L=50$ Å, where E_0^{gs} is clearly a slowly varying function of the E electric field [see Fig. 6(a)], to $L=500$ Å, where E_0^{gs} is a strongly varying function of E [see Fig. 6(d)], may be understood as follows. For narrow QWs ($L/2 \ll l_B$), the potentials associated to the electron and hole magnetic parabolas in Eq. (8) may be considered as a small perturbation, and the first-order eigenvalue E_0 [see Eq. (9)] of the Hamiltonian (8), corresponding to the $\eta=\alpha=0$ Landau magnetic subbands, is given by

$$E_0 = E_g + E_c - \frac{(eEl_B)^2}{2\beta_0} + \frac{1}{2}m_e^*\omega_e^2(z_e^0)^2 + \frac{1}{2}m_h^*\omega_h^2(z_h^0)^2,$$

$$(26)$$

where E_c is an electric-field independent constant and E_g is the GaAs gap, which must be added to Eq. (9) to have the correct expression for the noncorrelated *e-h* transition energy. It is easy to show now that the minimum value of E_0 in Eq. (26), for a fixed $\Delta=z_e^0-z_h^0$, is exactly $E_0=E_g+E_c$. This result, obtained in first-order approximation, and the fact that the higher-order correction to E_0 in Eq. (26) are relatively small, explain why the noncorrelated *e-h* transition energy is a slowly varying function of the applied electric field for $L=50$ Å, as shown in Fig. 6(a), for in-plane magnetic field ranging between $B=4$ T and $B=20$ T. Note that in this range
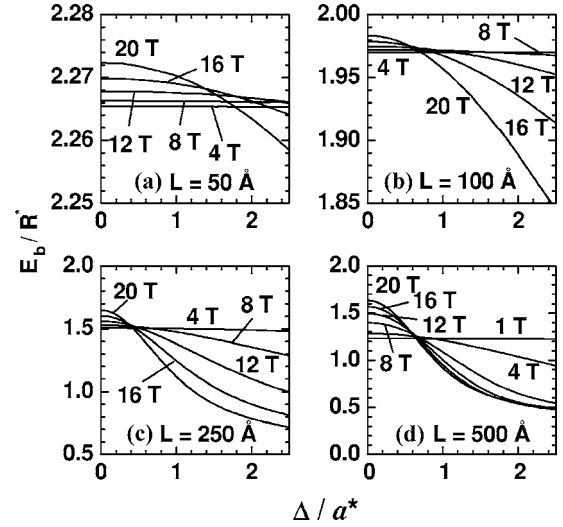
of magnetic-field values, the Landau length varies from $l_B=128$ Å (for $B=4$ T) to $l_B=57$ Å (for $B=20$ T), and therefore ($L/2=25$ Å $\ll l_B$). Moreover, as the GaAs/Ga$_{1-x}$Al$_x$As QW width is increased and becomes of the order of Landau length l_B, it is not anymore possible to apply perturbation theory and both the QW and magnetic potentials play similar roles in the determination of the electric-field dependence of E_0^{gs}. However, in the limit of wide GaAs/Ga$_{1-x}$Al$_x$As QWs ($L/2 \gg l_B$), the barrier-potential effects on the electron (hole) states are extremely small when the distance between the center $z_e^0(z_h^0)$ of the electron (hole) magnetic parabola and the QW edges situated at $z=\pm L/2$ is appreciable greater that the Landau length l_B. This means that the noncorrelated magnetic subband $E_0^e(z_0^e)$ $[E_0^h(z_0^h)]$ is essentially flat as a function of $z_e^0(z_h^0)$ for the mentioned distance, and therefore the electric-field dependence of the noncorrelated *e-h* transition energy E_0^{gs} is essentially determined by the fourth term in Eq. (9). This result explains the strong dependence of E_0^{gs} on the electric field shown in Fig. 6(d). Thus the transition from the regime where the QW potential effects dominate to the regime where these effects are negligibly small explains the evolution of the noncorrelated *e-h* energy transition with the growth-direction applied electric field.

The heavy-hole E_b exciton binding energy is shown in Fig. 7 as a function of the spatial distance Δ between the centers of the electron- and heavy-hole magnetic parabolas, for GaAs/Ga$_{0.7}$Al$_{0.3}$As QWs of different L well widths, and for various values of the in-plane magnetic field B. The relation between the corresponding growth-direction applied electric field E and K_y CM momentum, for fixed values of Δ and B, is determined by Eq. (11). As the fundamental pur-
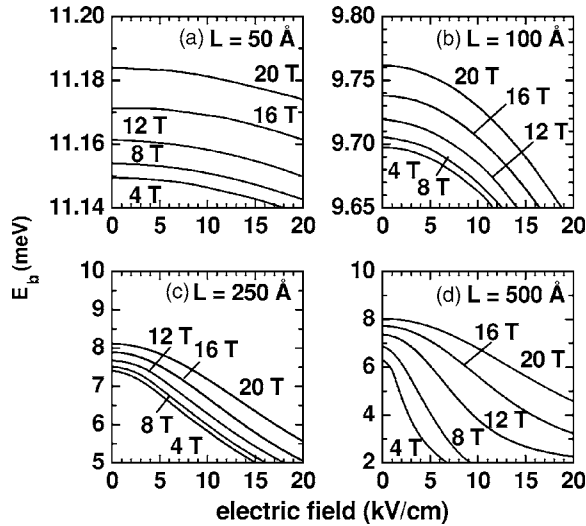
FIG. 8. Heavy-hole exciton binding energy as a function of the growth-direction applied electric field, for GaAs/Ga$_{0.7}$Al$_{0.3}$As QWs of different L well widths, $K_y=0$, and various values of the in-plane magnetic field.

pose of our discussion is to study the barrier-potential effects on the Δ dependence of E_b, we first note that the results depicted in Fig. 7(d), for an $L=500$-Å GaAs/Ga$_{0.7}$Al$_{0.3}$As QW, is essentially the same as those displayed in Fig. 2(a) for bulk GaAs. This is the result expected for finite values of Δ and sufficiently wide QWs. Another expected result, clearly seen in Figs. 7(a)–7(c), is the increase of E_b as the confinement effect associated to the QW increases, i.e., as the QW width L decreases. Note also that, as the QW width L decreases, E_b tends progressively towards a slow function of Δ, which becomes essentially flat for $L=50$ Å and for the lowest magnetic fields considered [see Fig. 7(a)]. These fields correspond to Landau lengths $l_B \gg L/2$, i.e., to the case of narrow QWs considered above. This result may be understood if one takes into account that, for $l_B \gg L/2$ and $z_{h,m}^0 = z_{e,m}^0 - \Delta$ localized inside the QW, the effect of the magnetic field is weak and the exciton binding-energy structure is essentially dominated by the barrier confining potential. For $l_B \gg L/2$ and $z_{h,m}^0 = z_{e,m}^0 - \Delta$ localized outside the QW, but finite, the E_b dependence on Δ is essentially flat because the effect of the magnetic field is still weak, and the average e-h distance along the z axis practically does not vary due to the fact that the electron and hole are localized, respectively, around $z_e \sim 0$ [see comment after Eq. (25)] and $z_h \sim -L/2$. In this last case, the localization of the hole around $z_h \sim -L/2$, and not around the center $z_{h,m}^0$ of the hole magnetic parabola, is due to the fact that the combined action of the barrier potential and the magnetic potential, for $z_{h,m}^0 < -L/2$, creates a second well with the minimum at $z_h \sim -L/2$. Since the confinement effects associated to this second well increases with the magnetic field, the e-h overlap decreases and therefore the corresponding exciton binding energy must decrease with Δ for $z_{h,m}^0 < -L/2$, as shown in Figs. 7(a)–7(c).

We display in Fig. 8 the heavy-hole E_b exciton binding energy as a function of the growth-direction applied electric field E, for GaAs/Ga$_{0.7}$Al$_{0.3}$As QWs of different L well widths, $K_y=0$, and various values of the in-plane magnetic

field B. In this case, the relation between E, B, and the spatial distance Δ between the centers of the magnetic parabolas is displayed in Fig. 1 and may be expressed as $\Delta \sim E/B^2$ or $E \sim B^2 \Delta$. Let us first of all consider the results shown in Fig. 8(d), for a GaAs/Ga$_{0.7}$Al$_{0.3}$As QW of $L=500$ Å well width. As this system corresponds to a relatively wide QW, it is useful to compare these results with those displayed (and already discussed) in Fig. 2(b) for bulk GaAs. One sees that, in the range of electric fields and exciton binding energies considered, the curve associated to the lowest magnetic field ($B=4$ T) in Fig. 8(d) exhibits a behavior clearly different from the corresponding one in Fig. 2(b). It is also clear that these differences tend progressively to disappear as the magnetic field increases. Notice, for instance, that for $B \gtrsim 8$ T, the corresponding results in both Figs. 2(b) and 8(d) may be considered essentially the same. The above described behavior of the exciton binding energy in an $L=500$-Å wide GaAs/Ga$_{0.7}$Al$_{0.3}$As QW, as compared to those of bulk GaAs, is determined, of course, by the barrier-potential effects. In fact, when the growth-direction applied electric field E is increased from zero, these effects first affect the curves associated to the lowest magnetic fields B as the E dependence of the Δ parameter, for fixed values of the magnetic field, is stronger than the corresponding one for higher magnetic fields [see Fig. 1(a)], and the carriers (electron and hole) are less confined for low values of the magnetic fields. The rapid increase of Δ with E, for $B=4$ T, also explains the rapid decrease of the corresponding exciton binding energy as E increases [see Fig. 8(d)]. Moreover, notice now, for instance, that, for $B=20$ T, the Δ parameter varies from 0 to 100 Å [see Fig. 1(a)] when the electric field goes from 0 to 20 kV/cm, and therefore $\Delta \ll L=500$ Å. This result, together with the strong confinement of the carriers (electron and hole) by this magnetic field, imply that the barrier-potential effects on the carriers are very weak and may be neglected in a first approximation, which explains why the results shown in Figs. 8(d) and 2(b) are essentially the same for $B=20$ T. Similar considerations may be used for other values of the magnetic field. Of course, these barrier-potential effects tend to disappear when L further increases. An expected result, clearly seen in Fig. 8, is the increase of E_b as the confinement effects associated to the QW and to the magnetic field increase, i.e., as the QW width L decreases and/or magnetic-field strength B increases. Note also that, as the QW confinement increases, E_b tends progressively towards a slow function of the applied electric field, which is due to the fact that, for sufficiently narrow QWs, the barrier-potential effects dominate.

The electric-field dependence of the PL exciton peak energies, or correlated e-h transition energies $E_X = E_0^{gs} - E_b$, is shown in Fig. 9 for GaAs/Ga$_{0.7}$Al$_{0.3}$As QWs of different L well widths, $K_y=0$, and various values of the applied magnetic field. Results presented in Fig. 9(d), for a QW of $L=500$-Å well width, are compared with those of bulk GaAs, shown as dotted lines. Note first that, in the range of growth-direction applied electric field considered, (0, 20 kV/cm), the spatial distance Δ between the centers of the magnetic parabolas takes values [see Fig. 1(a)] in the intervals (0, 2900 Å), for $B=4$ T; (0, 720 Å), for $B=8$ T; (0, 320 Å), for $B=12$ T; (0, 180 Å), for $B=16$ T; and (0, 120 Å), for B
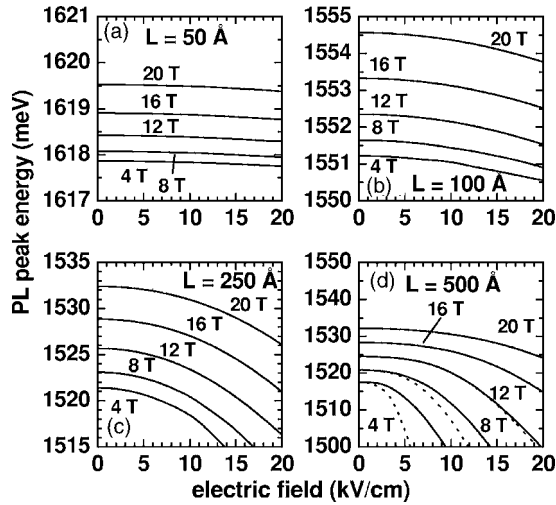
FIG. 9. PL peak energy (or correlated e-h energy transition) as a function of the growth-direction applied electric field, for GaAs/Ga$_{0.7}$Al$_{0.3}$As QWs of different L well widths, $K_y=0$, and various values of the in-plane applied magnetic field. Results for bulk GaAs are also shown as dotted lines in (d).

FIG. 10. PL peak energy (or correlated e-h energy transition) for an $L=200$ Å GaAs/Ga$_{0.7}$Al$_{0.3}$As QW, as a function of the in-plane applied magnetic field, for $K_y=0$, and different values of the growth-direction applied electric fields (1: $E=0$ kV/cm; 2: $E=5$ kV/cm; 3: $E=10$ kV/cm; 4: $E=15$ kV/cm; 5: $E=20$ kV/cm).

$=20$ T. From these values, and the confinement of the carriers (electron and hole) by the magnetic field, it is obvious that only the curves associated to low and moderate strengths of the magnetic field can be affected by the barrier-potential effects. This is clearly seen in Fig. 9(d), for $B=4$ T and $B=8$ T. The $B=12$-T curve is only slightly affected in the part corresponding to high values of the electric field; and the curves associated to higher magnetic fields, i.e., $B=16$ T and $B=20$ T, are essentially the same as the corresponding ones for bulk GaAs. Of course, these last curves may be affected by barrier-potential effects, for electric field E of sufficiently large strength, i.e., for $E>>20$ kV/cm. The interpretation of the remainder results depicted in Fig. 9, where the PL exciton peak energy increases with confinement effects (with decreasing L and increasing B), and tends progressively towards a slow function of the electric field, as the QW confinement increases, is similar to the interpretation given above in relation with Figs. 6–8.

In Fig. 10, we present our results for the PL peak energy for an $L=200$ Å GaAs/Ga$_{0.7}$Al$_{0.3}$As QW, as a function of the in-plane applied magnetic field, for $K_y=0$, and different values of the growth-direction applied electric fields, i.e.,

$$E_{PL} = E_g - \frac{(eEl_B)^2}{2\beta_0} + E^e_{\eta=0}(z^0_e) + E^h_{\alpha=0}(z^0_h) - E_b, \quad (27)$$

where E_g corresponds to the GaAs band-gap energy. For a fixed value of B (see the different curves in Fig. 10) and increasing values of the applied electric field, one has a decrease in the e-h binding energy as the polarization of the e-h wave function increases, and a decrease in the energies of the e-h noncorrelated pair. These two effects lead to a blueshift or a redshift, respectively, of the PL peak energy. As the width of the GaAs/Ga$_{0.7}$Al$_{0.3}$As QW is quite large ($L=200$ Å) the decrease in the energies of the e-h noncorrelated pair (under growth-direction applied electric fields) is
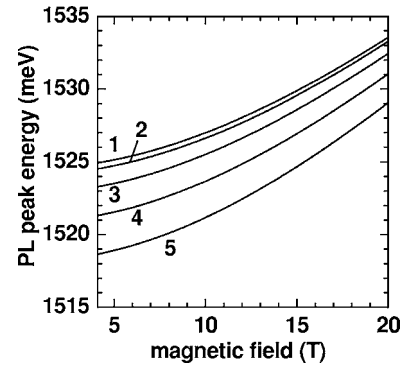
clearly the dominant effect, and one should obtain a redshift effect on the PL peak for fixed values of the magnetic field and increasing strengths of the applied electric field. On the other hand, for a fixed value of the growth-direction electric field, increasing confining effects with increasing values of the applied magnetic field lead to an increase in the e-h overlap and to a larger exciton binding energy, and would result in a redshift of the PL peak energy. Of course, again there is a competing effect from the increase in the energy of the e-h noncorrelated pair due to the magnetic-field effects on the electron and hole Landau electronic states, and this effect is the dominant one as the value of magnetic field increases, which leads to a blueshift of the PL peak energy, as expected. In Fig. 11, present theoretical results, in the absence of the applied electric field ($E=0$), and for $K_y=0$, for the magnetic-field-dependent diamagnetic shift of the PL peak position, for an $L=200$-Å GaAs/Ga$_{0.7}$Al$_{0.3}$As QW, are compared, with fair agreement, with recent experimental data by Ashkinadze *et al.*[12] Note that one could argue that, for high values of the applied magnetic field, a reliable calculation should involve a more realistic type of wave function which would appropriately take into account magnetic-field induced anisotropic effects. In that respect, we have
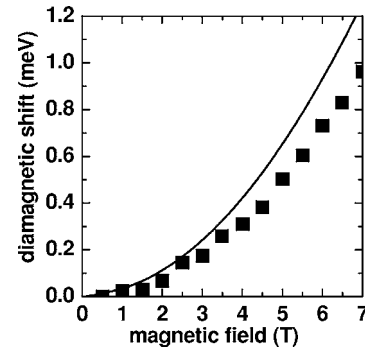

FIG. 11. Diamagnetic shift of the PL peak position for an $L=200$ Å GaAs/Ga$_{0.7}$Al$_{0.3}$As QW, in the absence of the applied electric field ($E=0$), and $K_y=0$, calculated as a function of the in-plane applied magnetic field, compared with the experimental measurements (full squares) by Ashkinadze *et al.* (Ref. 12).
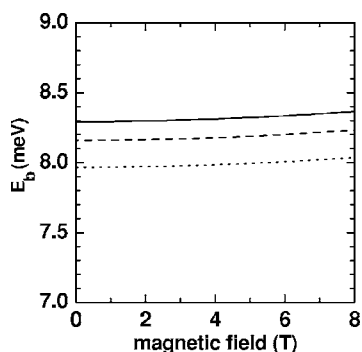
FIG. 12. Heavy-hole exciton binding energies, in the absence of the applied electric field ($E=0$) and $K_y=0$, as a function of the in-plane applied magnetic field, for an $L=200$ Å GaAs/Ga$_{0.7}$Al$_{0.3}$As QW. The dotted line corresponds to the exciton binding energy calculated by using $f(\vec{r}) \propto e^{-\lambda r}$, i.e., a one-parameter variational hydrogenic 1s-like wave function in Eqs. (12) and (13) for the exciton trial envelope variational wave function, whereas the dashed and full curves represent calculations with two- and three-parameter variational wave functions, $f(\vec{r}) \propto e^{-\lambda r - \alpha \rho^2}$ and $f(\vec{r}) \propto e^{-\lambda r - \alpha \rho^2 - \beta z^2}$, respectively.

performed calculations, for an $L=200$-Å GaAs/Ga$_{0.7}$Al$_{0.3}$As QW, of the exciton binding energy with hydrogeniclike variational wave functions depending on one (λ), two (λ and α), and three (λ, α, and β) variational parameters,[37] i.e., we have taken the 1s-like wave function in Eq. (12) as $f(\vec{r}) \propto e^{-\lambda r}$, $f(\vec{r}) \propto e^{-\lambda r - \alpha \rho^2}$, and $f(\vec{r}) \propto e^{-\lambda r - \alpha \rho^2 - \beta z^2}$, respectively. Calculated results are displayed in Fig. 12, and theoretical values for the exciton binding energies, with different 1s-like wave functions, differ at most by 4% and, as the magnetic-field-dependent resulting curves are essentially parallel, it is clear that these changes in the exciton binding energies would not affect the diamagnetic shift displayed in Fig. 11. A better quantitative description of the experimental data would certainly require a more realistic description of the exciton wave function with combinations of the solutions corresponding to different QW confined states and Landau levels, and by taking into account nonparabolicity effects and modifications of the nature of the subband-level structure due to crossed applied electric and in-plane magnetic fields. Most probably, this would at the same time improve the quantitative result for the diamagnetic shift and produce a more general symmetry for the magnetoexciton states. In addition, for shallow QWs, the light-hole band should come into play, as its energy distance is comparable to the Larmor energy for high magnetic fields.

IV. CONCLUSIONS

In conclusion, in the present work we have performed a systematic study of the effects of crossed growth-direction electric and in-plane magnetic fields on the electronic and exciton properties of bulk GaAs and semiconductor GaAs/Ga$_{1-x}$Al$_x$As QWs. We have adopted the effective-mass and parabolic-band approximations, and the theoretical formulation we have presented allows a simple treatment of the combined effects of the applied crossed electric and magnetic fields on the electronic and exciton properties in bulk GaAs and semiconductor GaAs/Ga$_{1-x}$Al$_x$As QWs, with the direct coupling between the exciton CM and internal exciton motions dealt with through a simple Δ parameter representing the spatial distance between the centers of the electron and hole magnetic parabolas. The exciton properties were calculated by using a simple hydrogenlike variational envelope excitonic wave function and therefore calculated results should be viewed as only qualitatively if confinements effects due to the in-plane magnetic or electric fields are comparable or larger than the spatial QW-barrier confinement. Present theoretical results, for low values of the in-plane applied magnetic field, were found in fair agreement with recent experimental measurements by Ashkinadze *et al.*[12] on the dependence of the exciton PL peak on applied in-plane magnetic fields. Of course, the present theoretical framework may be used with more sophisticated and reliable exciton variational wave functions, if one is interested in a more realistic description of the excitonic properties. Moreover, the present approach could be readily extended in order to treat optoelectronic properties in modulation-doped single and multiple QWs, QWWs, QDs, heterojunctions, superlattices, quasiperiodic superlattices, and essentially any other semiconductor heterostructures of interest.

[1] D. M. Whittaker, T. A. Fisher, P. E. Simmonds, M. S. Skolnick, and R. S. Smith, Phys. Rev. Lett. **67**, 887 (1991).

[2] M. Fritze, I. E. Perakis, A. Getter, W. Knox, K. W. Goossen, J. E. Cunningham, and S. A. Jackson, Phys. Rev. Lett. **76**, 106 (1996).

[3] L. V. Butov, A. V. Mintsev, Yu. E. Lozovik, K. L. Campman, and A. C. Gossard, Phys. Rev. B **62**, 1548 (2000).

[4] A. Parlangeli, P. C. M. Christianen, J. C. Maan, C. B. Soerensen, and P. E. Lindelof, Phys. Status Solidi A **178**, 45 (2000); A. Parlangeli, P. C. M. Christianen, J. C. Maan, I. V. Tokatly, C. B. Soerensen, and P. E. Lindelof, Phys. Rev. B **62**, 15323 (2000).

[5] M. Orlita, R. Grill, M. Zvára, G. H. Döhler, S. Malzer, M. Bysze-

wski, and J. Soubusta, Phys. Rev. B **70**, 075309 (2004).

[6] L. V. Butov, C. W. Lai, D. S. Chemla, Yu. E. Lozovik, K. L. Campman, and A. C. Gossard, Phys. Rev. Lett. **87**, 216804 (2001).

[7] L. V. Butov, J. Phys.: Condens. Matter **16**, R1577 (2004).

[8] D. Y. Oberli, G. Böhm, G. Weimann, and J. A. Brum, Phys. Rev. B **49**, 5757 (1994).

[9] J. Feldmann, G. Peter, E. O. Göbel, P. Dawson, K. Moore, C. Foxon, and R. J. Elliott, Phys. Rev. Lett. **59**, 2337 (1987).

[10] R. Houdré, C. Weisbuch, R. P. Stanley, U. Oesterle, P. Pellandini, and M. Ilegems, Phys. Rev. Lett. **73**, 2043 (1994).

[11] A. Tredicucci, Y. Chen, V. Pellegrini, M. Börger, L. Sorba, F. Beltram, and F. Bassani, Phys. Rev. Lett. **75**, 3906 (1995).

[12] B. M. Ashkinadze, E. Linder, E. Cohen, and L. N. Pfeiffer, Phys. Rev. B **71**, 045303 (2005).

[13] L. P. Gorkov and I. E. Dzyaloshinskii, Zh. Eksp. Teor. Fiz., **53**, 717 (1967) [Sov. Phys. JETP **26**, 449 (1968)].

[14] D. Paquet, T. M. Rice, and K. Ueda, Phys. Rev. B **32**, 5208 (1985).

[15] M. M. Dignam and J. E. Sipe, Phys. Rev. B **45**, 6819 (1992).

[16] A. Imamoglu, Phys. Rev. B **54**, R14285 (1996).

[17] Yu. E. Lozovik and A. M. Ruvinskii, Zh. Eksp. Teor. Fiz. **112**, 1791 (1997) [JETP **85**, 979 (1997)]; Yu. E. Lozovik, I. V. Ovchinnikov, S. Yu. Volkov, L. V. Butov., and D. S. Chemla, Phys. Rev. B **65**, 235304 (2002); Yu. E. Lozovik and S. Yu. Volkov, Zh. Eksp. Teor. Fiz. **123**, 635 (2003) [JETP **96**, 564 (2003)].

[18] A. A. Gorbatsevich and I. V. Tokatly, Semicond. Sci. Technol. **13**, 288 (1998).

[19] Kai Chang and F. M. Peeters, Phys. Rev. B **63**, 153307 (2001).

[20] Kai Chang, J. B. Xia, H. B. Wu, and S. L. Feng, Appl. Phys. Lett. **80**, 1788 (2002).

[21] K. Chang, D. S. Jiang, and J. B. Xia, J. Appl. Phys. **95**, 752 (2004).

[22] N. E. Kaputkina and Yu. E. Lozovik, Physica E (Amsterdam) **12**, 323 (2002).

[23] E. C. Niculescu, Superlattices Microstruct. **33**, 103 (2003).

[24] E. Reyes-Gómez, L. E. Oliveira, and M. de Dios-Leyva, Phys. Rev. B **71**, 045316 (2005).

[25] G. Coli and K. K. Bajaj, Phys. Rev. B **61**, 4714 (2000).

[26] A. Antonelli, J. Cen, and K. K. Bajaj, Semicond. Sci. Technol. **11**, 74 (1996).

[27] A. Latgé, N. Porras-Montenegro, M. de Dios-Leyva, and L. E. Oliveira, Phys. Rev. B **53**, 10160 (1996); L. H. M. Barbosa, A. Latgé, M. de Dios-Leyva, and L. E. Oliveira, Solid State Commun. **98**, 215 (1996); F. J. Ribeiro, A. Latgé, and L. E. Oliveira,

J. Appl. Phys. **80**, 2536 (1996); A. Latgé, N. Porras-Montenegro, M. de Dios-Leyva, and L. E. Oliveira, Phys. Status Solidi B **210**, 655 (1998).

[28] A. Latgé, N. Porras-Montenegro, and L. E. Oliveira, Phys. Rev. B **45**, 6742 (1992); L. E. Oliveira, N. Porras-Montenegro, and A. Latgé, *ibid.* **47**, 13864 (1993).

[29] C. A. Duque, C. L. Beltrán, A. Montes, N. Porras-Montenegro, and L. E. Oliveira, Phys. Rev. B **61**, 9936 (2000).

[30] E. Herbert Li, Physica E (Amsterdam) **5**, 215 (2000).

[31] It is clear that the inclusion of the electron and hole mass mismatches as well as the dielectric constant mismatch in the barriers are important, especially in the regime of small widths ($L \lesssim 100$ Å) of the GaAs/Ga$_{1-x}$Al$_x$As QW. For example, for a well width of 50 Å, the dielectric constant mismatch gives origin to a larger binding energy by ~ 1 meV, whereas inclusion of the mass mismatches diminishes the binding energy by ~ 1 meV, and the combined effect of mass and dielectric constant mismatches essentially leaves the exciton binding energy unaltered (Ref. 32). Here therefore we have considered the electron and hole effective masses as well as the dielectric constant as constants and equal to the values in GaAs throughout the heterostructure.

[32] B. Gerlach, J. Wüsthoff, M. O. Dzero, and M. A. Smondyrev, Phys. Rev. B **58**, 10568 (1998).

[33] Here we note that the assumption of the above separable exciton trial wave function introduces some limitations in the validity of calculated results. For a QW in the presence of crossed electric and in-plane magnetic fields, confinement is a complicate competition between wave-function compression provided by the magnetic field, the electric-field induced polarization, and the barrier-potential effects. By choosing a simple hydrogenlike envelope excitonic wave function, one would therefore expect a quantitatively realistic description of the exciton properties only in semiconductor heterostructures in which the spatial and barrier-potential confinement dominates and/or confinement effects due to the electric and in-plane magnetic applied fields are at most moderate.

[34] J-B. Xia and W-J. Fan, Phys. Rev. B **40**, 8508 (1989).

[35] M. de Dios-Leyva, A. Bruno-Alfonso, and L. E. Oliveira, J. Phys.: Condens. Matter **9**, 1005 (1997).

[36] E. Reyes-Gómez, A. Matos-Abiague, C. A. Perdomo-Leiva, M. de Dios-Leyva, and L. E. Oliveira, Phys. Rev. B **61**, 13104 (2000).

[37] S. Chaudhuri and K. K. Bajaj, Solid State Commun. **52**, 967 (1984); Phys. Rev. B **29**, 1803 (1984).